

Article

Effect of Temperature on the Microwave-Absorbing Properties of an Al₂O₃–MoSi₂ Coating Mixed with Copper

Cheng Gao ^{1,2}, Yangsheng Jiang ², Dayong Cai ^{1,*}, Jinyong Xu ² and Weiyao Xiao ²

¹ College of Materials Science and Engineering, Yanshan University, No. 438 West Hebei Avenue, Qinhuangdao 066004, China; cgao1982@126.com

² School of Mechanical and Electrical Engineering, Guilin University of Electronic Technology, No. 1 of Jinji Road, Guilin 541004, China; bobi6658@hotmail.com (Y.J.); xujinyong62@163.com (J.X.); xiaoweiyao2017@126.com (W.X.)

* Correspondence: cdy@ysu.edu.cn

Abstract: To obtain a high temperature-resistant microwave absorbing coating, an Al₂O₃–MoSi₂/Cu composite coating was prepared by atmospheric plasma spraying. Compared with a normal temperature environment, there are a few reports on Cu as an absorbent for high temperature microwave absorbing coatings. Therefore, in this regard, wave absorbing property can be improved by using a Cu absorbent. The microstructure of a Al₂O₃–MoSi₂/Cu coating was observed, and the dielectric properties of the composite coating in the high-temperature environment of the X-band were tested. The experimental results show that with the increase in temperature, Cu transforms Cu₂O in the high-temperature environment and improves the coating's wave absorption performance with MoSi₂. In addition, a 1.4 mm-thick coating showed best microwave absorbing performance at 700 °C. The reflection loss was –19.09 dB, and the effective microwave absorbing bandwidth was 2.83 GHz (Reflection Loss < –10 dB). It was found that the Al₂O₃–MoSi₂/Cu composite coating has good wave-absorbing performance in a 700 °C high-temperature environment.

Keywords: atmospheric plasma spraying; microwave absorption coating; high-temperature; Cu



Citation: Gao, C.; Jiang, Y.; Cai, D.; Xu, J.; Xiao, W. Effect of Temperature on the Microwave-Absorbing Properties of an Al₂O₃–MoSi₂ Coating Mixed with Copper. *Coatings* **2021**, *11*, 940. <https://doi.org/10.3390/coatings11080940>

Academic Editor: Douglas Wolfe

Received: 22 June 2021

Accepted: 3 August 2021

Published: 5 August 2021

Publisher's Note: MDPI stays neutral with regard to jurisdictional claims in published maps and institutional affiliations.



Copyright: © 2021 by the authors. Licensee MDPI, Basel, Switzerland. This article is an open access article distributed under the terms and conditions of the Creative Commons Attribution (CC BY) license (<https://creativecommons.org/licenses/by/4.0/>).

1. Introduction

Recent studies have shown that due to radar detection technology's rapid development, an increasing amount of attention has been paid to radar stealth technology research. Meanwhile, an increasing number of researchers have investigated high-temperature microwave absorbing materials [1–9]. The high-temperature absorbing coating prepared by the plasma spraying method has good absorbing performance [10–13]. Al₂O₃ and MoSi₂ are widely used in high-temperature resistant coatings due to their excellent high-temperature resistance [14–16]; Cu is rarely studied in a high-temperature environment as an absorbing material.

As an electromagnetic wave absorber, MoSi₂ powder has certain characteristics—high melting point, low relative density, and excellent high-temperature oxidation resistance—and is widely used in high temperature-resistant coating materials, composite materials, and high temperature-resistant structures [17]. Researchers have carried out in-depth studies on the wave absorption performance and high-temperature oxidation of MoSi₂. This research used MoSi₂–30Al₂O₃ as raw a material, prepared a MoSi₂–Al₂O₃ electrothermal coating by atmospheric plasma spraying, and studied the electrothermal properties of the composite coating [18]. Shang et al. [19] prepared MoSi₂/BC porous composite microwave absorbing material by the solid-phase sintering method and found that it had good absorbing performance. When the MoSi₂/BC mass fraction was 50%, the reflection loss was the lowest; the effective absorption bandwidth of the microwave absorbing material was approximately 1.0 GHz, and the reflection loss was –13 dB. Jiao et al. [20] prepared a MoSi₂–CoNiCrAlY composite coating on the surface of a GH4169 alloy, and studied

the cyclic oxidation behavior of the composite coating under a 900 °C static atmosphere environment; they found that the composite coating has good high-temperature oxidation resistance. Wu et al. [21] prepared MoSi₂/Al₂O₃ coatings with different MoSi₂ contents by atmospheric plasma spraying; it was found that with the increase in MoSi₂ content, the electrical conductivity and dielectric loss of the coatings also increased.

Cu is an electromagnetic shielding material. Its electromagnetic shielding performance has been widely studied; it has good conductivity and wear resistance, and can thus be used as an effective absorbent in coatings. However, for the preparation of mixed high temperature-resistant microwave absorbing coatings, research is rare. Moustafa et al. [22] prepared copper–graphite composite materials with different graphite contents by powder metallurgy metohes and copper coating on graphite powder by the electroless coating technique. The results show that the graphite powder made by the two metohes has a lower wear rate and friction coefficient. Sun et al. [23] used the micro-arc discharge method for the synthesis of a carbon-coated copper nanocapsule made with Cu nanocapsule as the core and carbon absorbing material as the shell of the core-shell structure; the study found that the thickness of 1.9 mm of the carbon-coated copper nanocapsule and a reflection loss of −40 dB was achieved at 10.52 GHz. The carbon-coated copper nanocapsule has excellent absorbing performance. Zhao et al. [24], through a simple solution reduction method, made a new leaf-like NiCu alloy composite. The experiment discovered that 40 wt.% of NiCu has good microwave absorbing performance, since reflection loss reached −21.1 dB, and the microwave absorption bandwidth was 3.4 GHz.

In this research, both Al₂O₃ and MoSi₂ have good high-temperature stability and can be used in temperature environments. Therefore, an Al₂O₃–MoSi₂ composite coating was used as the substrate, and Cu particles were sprayed onto the surface of the Al₂O₃–MoSi₂ composite coating by plasma spraying. Cu in high-temperature microwave absorbing coatings is rarely studied; however, it has a lot of research value. In high-temperature environments with sufficient O₂, Cu is transformed into CuO [25] and Cu₂O [26], and the copper oxide formed by Cu transformation will improve the wave absorbing performance of the Al₂O₃–MoSi₂/Cu composite coating. An Al₂O₃–MoSi₂/Cu composite high-temperature absorbing coating was successfully prepared by atmospheric plasma spraying. The microstructure, composition, and dielectric properties of the Al₂O₃–MoSi₂/Cu composite coatings at different temperatures were summarized, and the wave absorption properties of three thickness coatings were researched at different temperatures. Therefore, this research provides a new insight into the preparation of high-temperature absorbing coatings.

2. Materials and Methods

An Al₂O₃–MoSi₂/Cu coating was prepared by the atmospheric plasma spraying method, and its high temperature microwave absorbing performance tested in the X-band. After the coating was finished by plasma spraying, the coating sample was cut into the size required by the instrument test. It was analyzed by X-ray diffraction (XRD, D8-Advance, Bruker, Bremen, Germany, Cu–K α radiation). The microstructure of the coating surface was observed by a scanning electron microscope (SEM, Quanta 450 FEG, FEI Company, Hillsboro, OR, USA), and the high-temperature electromagnetic and wave absorption properties of the coating were measured by a vector network analyzer (Agilent E8363B PNA, Santa Clara, CA, USA).

2.1. Preparation of Spraying Feedstock

MoSi₂ powder was produced by Shanghai Naiou Nanotechnology Co., Ltd. (Shanghai, China). The powder size was between 15 and 40 μ m, and the shape of MoSi₂ was irregular. Cu particles were produced by Shanghai Naiou Nano Technology Co., Ltd. (Shanghai, China). The size of Cu powder particles was different, with the large particle size ranging from 20 to 35 μ m and the small particle size ranging from 10 to 15 μ m. Al₂O₃ powder was produced by Shanghai Xiangtian Nanomaterials Co., Ltd. (Shanghai, China). The particle size of the powder was 30~60 μ m. MoSi₂ powder, Cu powder, and Al₂O₃ powder are

all micron powder, and micron-sized powder can be used to make the powder mixture uniform and powder feeding uniform in the spraying process. The raw powder content information is shown in Table 1.

Table 1. Al₂O₃–MoSi₂ mix particles and Cu particles of feedstock materials (wt. %).

Powder	Purity	Mo	Cu	Si	Fe	Ni	Fe ₂ O ₃	SiO ₂	Others
MoSi ₂	99.9	64.5	0.01	35.3	0.001	0.002	-	-	Bal.
Al ₂ O ₃	99.9	-	-	-	-	-	0.05	0.05	Bal.
Cu	99.9	-	99.8	-	0.01	0.05	-	-	Bal.

To mix Al₂O₃ and MoSi₂, the ball mill method was used at a speed of 380 r/min for 3.5 h, and appropriate alcohol was added. After ball milling, the mixed powder solution was poured into the container, placed into a blower, and the drying temperature was set at 90 °C. The Al₂O₃–MoSi₂ (80 wt% Al₂O₃ + 20 wt% MoSi₂) mixed powder was dried via an air dryer and grinded into a uniform and delicate powder using a mortar. The preparation process of Cu powder is the same as that of the Al₂O₃–MoSi₂ mixed powder. The mix powder phase of the samples was determined by X-ray diffraction in the 2θ range from 20 to 80°.

2.2. Plasma Spraying Experiment

Before plasma spraying, the substrate had to be pretreated, which included two processes: oil removal and sandblasting. The plasma spraying equipment included the SX-80, produced by Guangdong Sanxin Company (Guangzhou, China). In the spraying process, Al₂O₃–MoSi₂ mixed particles are first sprayed on the substrate. After the preparation of the Al₂O₃–MoSi₂ composite coating, 0.05 mm-thick Cu particles were sprayed onto the surface of the Al₂O₃–MoSi₂ coating. Ar was used as the main gas in plasma spraying as Ar is an inert gas that has an excellent protective effect on spraying particles, and Ar has a lower enthalpy and a faster temperature rise. H₂ is mainly used as a secondary gas. H₂ has excellent heat transferability, which is conducive to the refractory powder's melting and can prevent the spraying powder's oxidation. An SEM micrograph of the Al₂O₃–MoSi₂/Cu composite coating is shown in Figure 1, and the plasma spraying parameter settings are shown in Table 2.

Table 2. Atmosphere plasma spraying parameters.

Parameters	Value
Arc Current (A)	410
Arc Voltage (V)	30
Primary gas (Ar) flow rate (L/h)	2100
Secondary gas (H ₂) rate (L/h)	10
Spray distance (mm)	80
Powder carrier gas (Ar) flow rate (L/h)	200
Powder feed rate (g/min)	20

2.3. Dielectric Properties of the Coating

The Agilent E8363B PNA series vector network analyzer was used for the high-temperature wave absorption test. The electromagnetic parameters of the samples were tested by the wave-guide method [27] in the frequency range of 8.2 GHz–12.4 GHz (X-band). Before the test, the coating was cut into the sample holder with dimensions of 22.86 mm × 10.16 mm × 2 mm (X-band sample size); if the coating sample needed to be heated to more than 100 °C, heat preservation was done at 100 °C for 2 h, and then the dielectric constant of the coating was tested by E8363B from 25 °C to 700 °C in the X-band. The temperature of the waveguide increased at a rate of 10 °C per minute, monitored by a thermostat and software. The high temperature electromagnetic parameter test system is show in Figure 2.

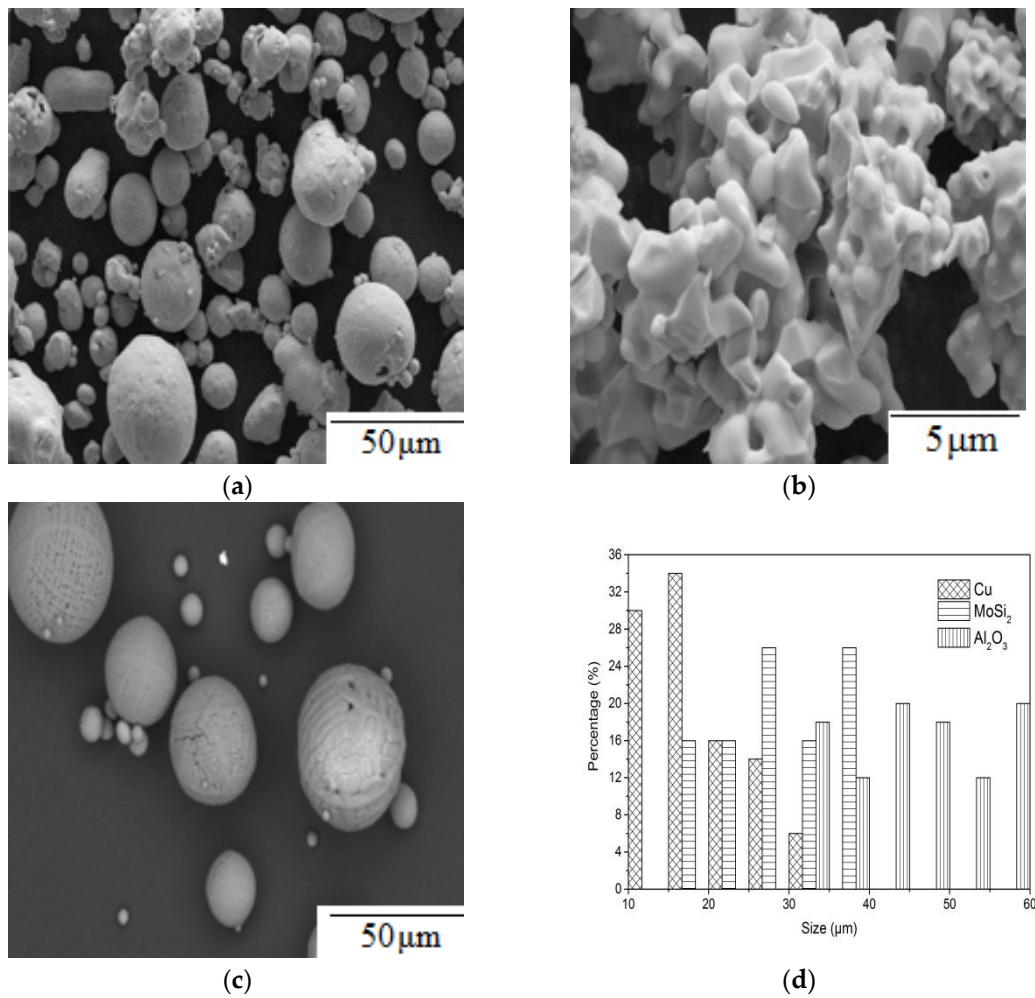


Figure 1. Three-elements distribution on the upper surface of the Al₂O₃–MoSi₂/Cu coating and feedstock: (a) Cu; (b) MoSi₂; (c) Al₂O₃; (d) the corresponding particle size distribution histograms of the Cu, MoSi₂, and Al₂O₃ particles.

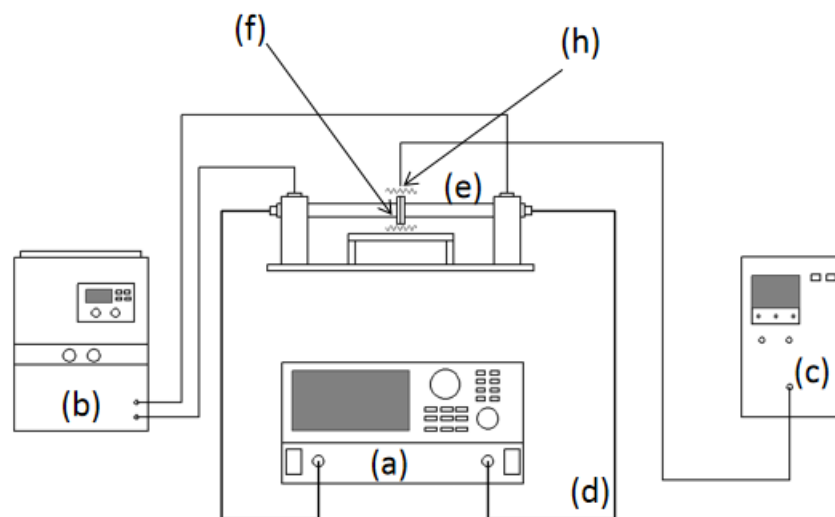


Figure 2. High-temperature electromagnetic parameter test system: (a) Vector network analyzer; (b) Cooling system; (c) thermostat; (d) Coaxial line; (e) Rectangular waveguide; (f) Sample; (h) Thermocouple.

The $\text{Al}_2\text{O}_3\text{-MoSi}_2/\text{Cu}$ coating is a dielectric microwave absorbing material, and its complex dielectric constant can be calculated by Equation (1) [28]:

$$\varepsilon_r = \varepsilon' - j\varepsilon'' \quad (1)$$

The reflection loss dB of the coating can be calculated by transmission line theory Equation (2) [29] and Equation (3) [30]:

$$R = 20 \lg \left| \frac{Z_{\text{in}} - Z_0}{Z_{\text{in}} + Z_0} \right| \quad (2)$$

$$Z_{\text{in}} = Z_0 \sqrt{\frac{\mu_r}{\varepsilon_r}} \tanh \left[j \left(\frac{2\pi f d}{c} \right) \sqrt{\mu_r \varepsilon_r} \right] \quad (3)$$

where ε_r of Equation (1) represents the complex dielectric constant of the material. Z_0 represents the air impedance of the microwave absorbing material, and Z_{in} represents the material's input impedance. In the formula, f represents the frequency of the electromagnetic wave, d represents the thickness of the material, c represents the speed of the electromagnetic wave uppropagation under vacuum, and j is an imaginary unit. $\text{Al}_2\text{O}_3\text{-MoSi}_2/\text{Cu}$ is a pure dielectric material, so μ_r in the formula is 1.

3. Results and Discussion

3.1. Microstructure of the Coating

The XRD analysis of the $\text{Al}_2\text{O}_3\text{-MoSi}_2$ powder is shown in Figure 3. It can be seen from the figure that the XRD of the particles is composed of MoSi_2 and $\alpha\text{-Al}_2\text{O}_3$, with many peaks of different degrees; the strongest peak is MoSi_2 . A new $\alpha\text{-Al}_2\text{O}_3$ phase was produced in the process of preparing $\text{Al}_2\text{O}_3\text{-MoSi}_2$ powder by ball milling. In addition, there were no new compounds. The XRD analysis of the Cu powder is shown in Figure 4. It can be seen from the figure that the peak of Cu is very sharp, and there is no peak of other elements, so the purity of the Cu powder is very high.

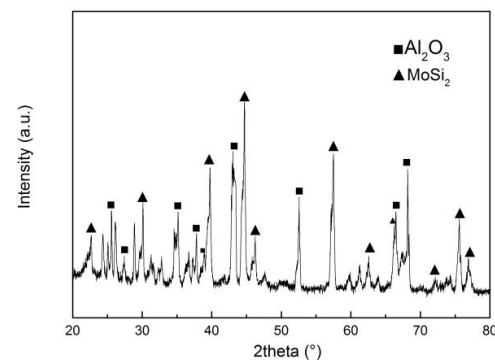


Figure 3. X-ray diffraction of the $\text{Al}_2\text{O}_3\text{-MoSi}_2$ mix powder.

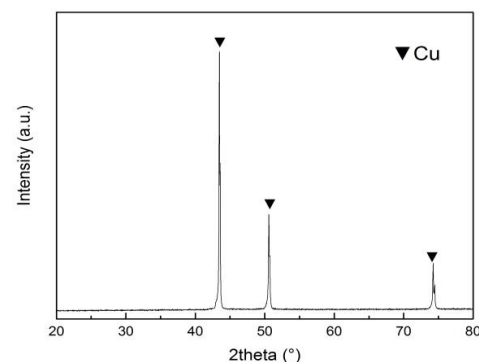


Figure 4. X-ray diffraction of the Cu powder.

The XRD analysis of the $\text{Al}_2\text{O}_3\text{-MoSi}_2/\text{Cu}$ composite coating is shown in Figure 5a. The coating is mainly composed of Al, O, Si, Mo, and Cu. By comparing the XRD of the powder and the coating, it can be seen that new phases of MoSi_2 and Cu are formed. The coating surface comprises of seven phases: MoSi_2 , Hex- MoSi_2 , Mo_5Si_3 , $\alpha\text{-Al}_2\text{O}_3$, $\gamma\text{-Al}_2\text{O}_3$, Cu, and Cu_2O . The sharpest peaks are Cu and $\alpha\text{-Al}_2\text{O}_3$, with different strength peaks caused by the powder's high temperature and oxidation during the plasma spraying. A small amount of new Cu_2O phase appeared in the coating as a small amount of oxygen entered the plasma flame during the spraying process, and part of the Cu powder was oxidized during the accelerated melting process, generating a Cu_2O new phase [31]. A small amount of Mo_5Si_3 and Hep- MoSi_2 appeared in the coating as MoSi_2 was mixed with a small amount of oxygen in the plasma spraying process [32]. The experiments show that the addition of Al_2O_3 to MoSi_2 could change the resistivity and low-temperature oxidation resistance of MoSi_2 [33]. This "peeling" is a coating defect as MoSi_2 at $400\text{--}600\text{ }^\circ\text{C}$ causes a phenomenon that transforms the material into powder; the addition of Al_2O_3 can prevent the rapid oxidation of the MoSi_2 phenomenon [34]. In the XRD analysis, the $\text{Al}_2\text{O}_3\text{-MoSi}_2/\text{Cu}$ composite coating was heated at $700\text{ }^\circ\text{C}$ and heat preservation for 0.5 h is shown in Figure 5b. CuO and SiO_2 appeared on the composite coating surface at $700\text{ }^\circ\text{C}$. CuO was produced as in the full reaction of Cu_2O with O_2 ; Cu_2O (inner layer) slowly converted to CuO (coating surface) [35]. SiO_2 generation is the full reaction of MoSi_2 with O_2 .

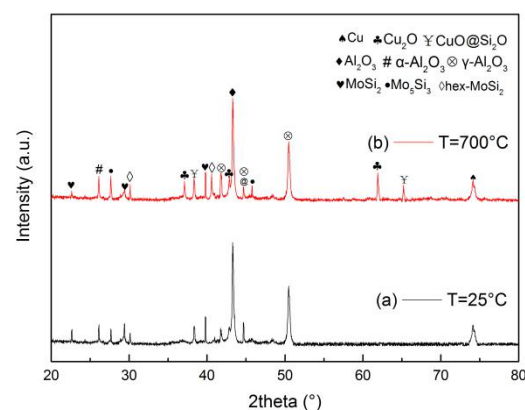


Figure 5. X-ray diffraction of the $\text{Al}_2\text{O}_3\text{-MoSi}_2/\text{Cu}$ composite coating surface: (a) $T = 25\text{ }^\circ\text{C}$ (b) $T = 700\text{ }^\circ\text{C}$.

Figure 6 shows the SEM micrograph of the $\text{Al}_2\text{O}_3\text{-MoSi}_2/\text{Cu}$ composite coating. It can be clearly seen that Cu, Al_2O_3 , and MoSi_2 particles are irregularly distributed on the coating surface, while there are a few pores on the coating surface.

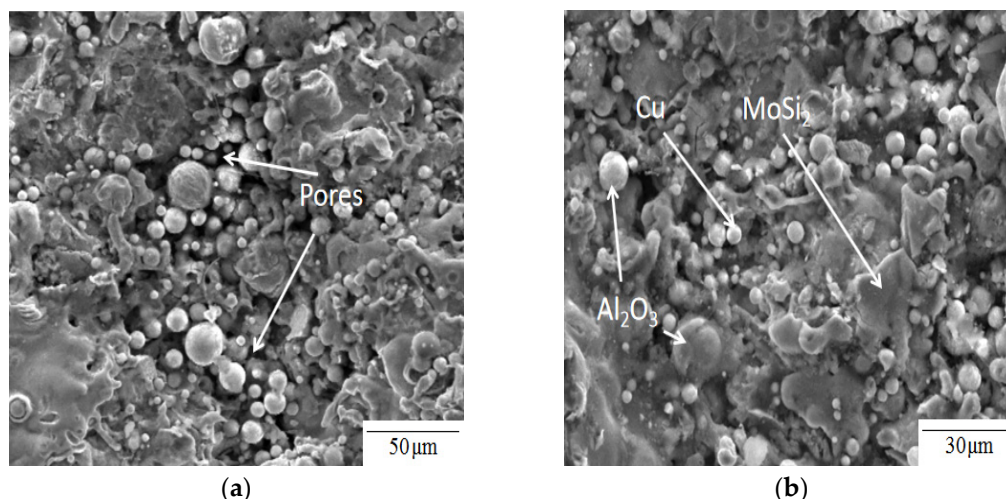


Figure 6. SEM micrographs of the $\text{Al}_2\text{O}_3\text{-MoSi}_2/\text{Cu}$ coating upper surface: (a) some pores exist in the coating surface (b) MoSi_2 , Al_2O_3 , and Cu particles.

3.2. Dielectric Properties of the Coating

As shown in Figure 7, the ϵ' and ϵ'' of the coating increased with the increase in temperature. The ϵ' and ϵ'' of the coating are 10.23 and 2.11 at 25 °C, 13.1 and 3.55 at 200 °C, and 22.4 and 5.09 at 500 °C, respectively. The dielectric constant of the Al₂O₃-MoSi₂/Cu coating changed with the increase in temperature. It can be seen from Figure 7a that the ϵ' increased with the increase in temperature. At two different temperature ranges in 200 °C and 600 °C, we can find that the ϵ' gradually moved to the high-frequency range. ϵ' at a high temperature can be expressed by Debye's theory in Equation (4) [36]:

$$\epsilon' = \epsilon_{\infty} + \frac{\epsilon_S - \epsilon_{\infty}}{1 + [\omega\tau(T)]^2} \quad (4)$$

where ϵ_{∞} is the limit value of the permittivity changing with the increase in ω , ϵ_S is the static permittivity, and $\tau(T)$ is the relaxation period. The relationship between relaxation time and temperature can be expressed by the Arrhenius formula in Equation (5) [37]:

$$\tau(T) = \tau_0 \exp\left(\frac{E_a}{RT_0}\right) \quad (5)$$

where E_a is the activation energy, τ_0 is the pre-factor, and T_0 is the temperature. R is Avogadro's constant.

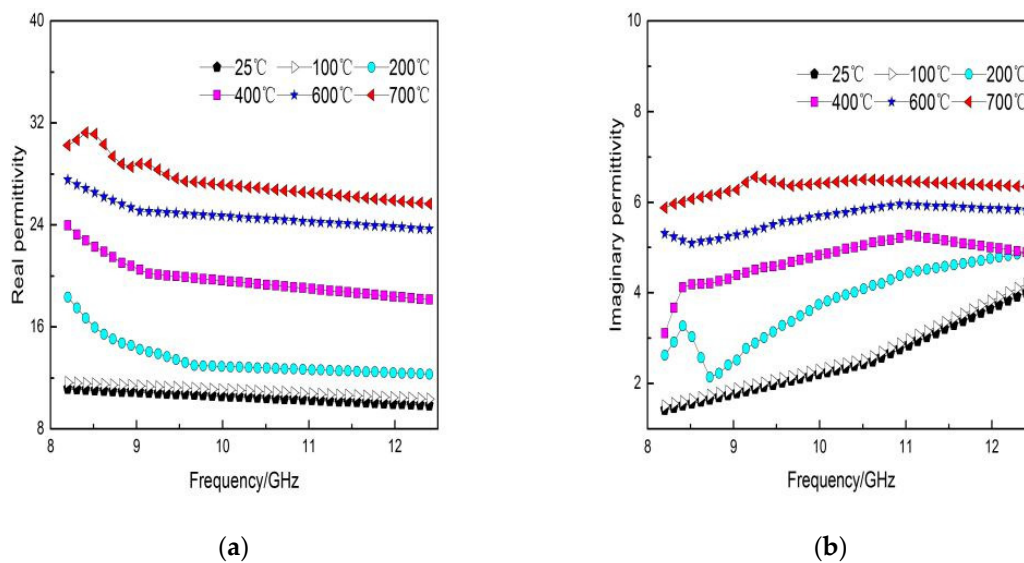


Figure 7. Dielectric properties of the Al₂O₃-MoSi₂/Cu composite coating: (a) ϵ' of the Al₂O₃-MoSi₂/Cu composite coating; (b) ϵ'' of the Al₂O₃-MoSi₂/Cu composite coating.

As shown in Figure 7b, ϵ'' also increases with the material temperature. The material was tested at two different temperatures of 200 and 600 °C, showing that the higher the temperature, the lower the relaxation time. At a high temperature, ϵ'' can be expressed in Equation (6) [36]:

$$\epsilon'' = \epsilon_{\infty} + \frac{(\epsilon_S - \epsilon_{\infty})\omega\tau(T)}{1 + \omega^2[\omega\tau(T)]^2} + \frac{\sigma(T)}{\omega\epsilon_0} \quad (6)$$

where $\sigma(T)$ is the conductivity of the medium, and the ϵ' and ϵ'' of the Al₂O₃-MoSi₂/Cu increased gradually with the increase in temperature. ϵ' moved from the low-frequency region to the high-frequency region with increased temperature, and ϵ' decreased with the frequency increase. This phenomenon is called the dispersion effect [38]. This may be due to the formation of a conductive network between MoSi₂ and Al₂O₃ [39], and the increase in temperature led to an increase in the conductivity of Al₂O₃-MoSi₂/Cu and the enhancement of conduction loss. ϵ'' moved from the low-frequency region to the high-

frequency region with the increase in temperature. The main effect is that the increase in temperature led to the coating's improved electrical conductivity [40]. Additionally, it can be seen from Figure 6 that the relaxation time became shorter as the temperature increased and that the real and imaginary parts of the complex dielectric constant of the $\text{Al}_2\text{O}_3\text{-MoSi}_2/\text{Cu}$ coating were lower at 25 °C. The $\text{Al}_2\text{O}_3\text{-MoSi}_2/\text{Cu}$ coating has remarkable dielectric properties at high temperatures.

3.3. Absorbing Performance of the Coating

The wave absorption performances of the coatings are shown in Figure 8. According to transmission line theory Equations (2) and (3), the absorption peak frequency of the 1.0 mm-thick coating was 11 GHz, and the reflection loss was -11.69 dB. When the coating reached 700 °C, the wave absorption performance was the best. The lowest of the 1.2 mm coating frequency was 10.8 GHz, and the reflection loss was -14.87 dB. When the coating's temperature reached 700 °C, the wave absorption performance was the best. The thickness of the coating was 1.4 mm, the frequency of the best absorption performance was in 10.51 GHz, the reflection loss was -19.09 dB, and the absorption performance was the best when the temperature reached 700 °C. It can be seen that the $\text{Al}_2\text{O}_3\text{-MoSi}_2/\text{Cu}$ coating has good high-temperature wave absorbing performance.

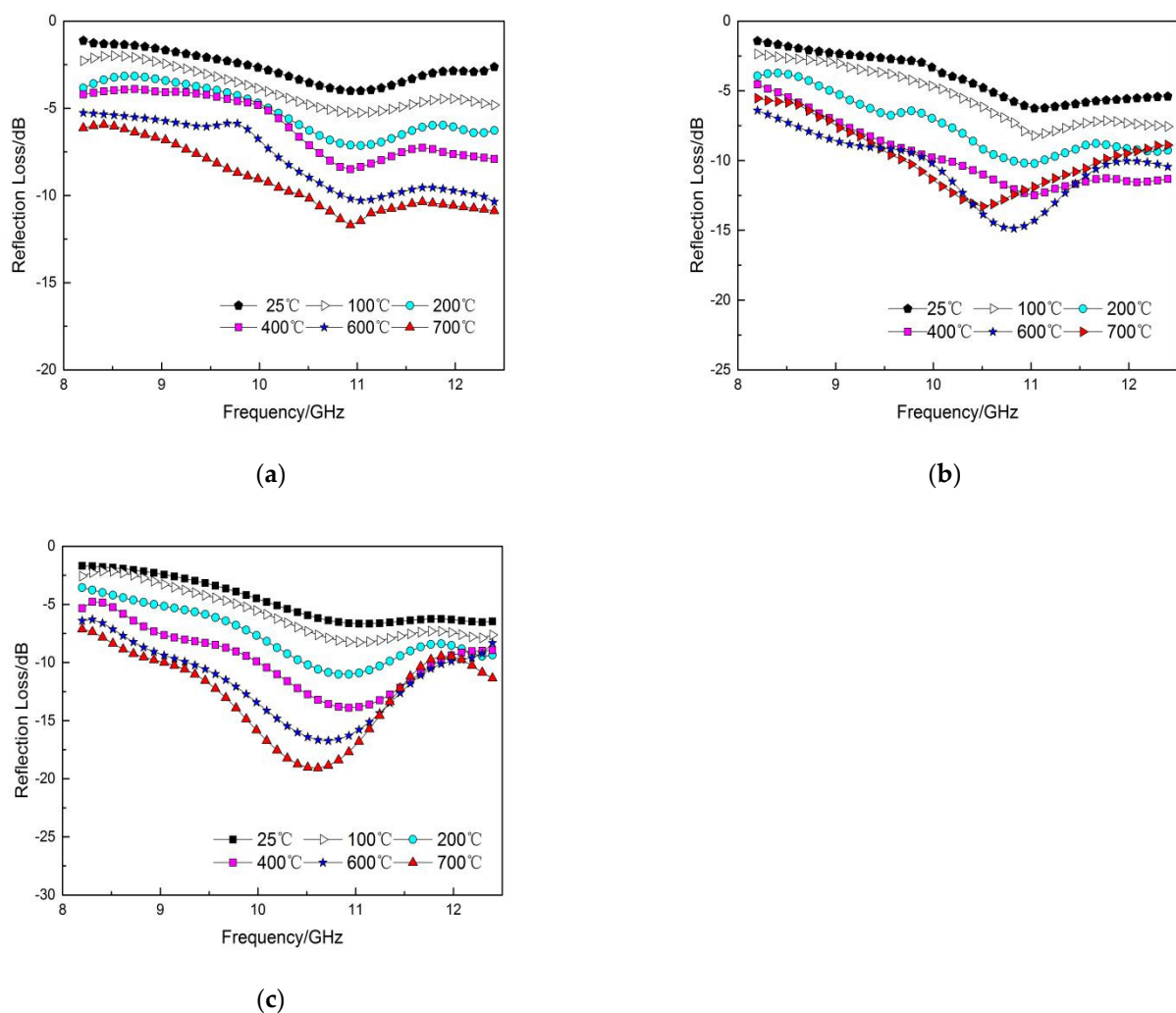


Figure 8. Reflection loss of the $\text{Al}_2\text{O}_3\text{-MoSi}_2/\text{Cu}$ composite coatings: (a) $d = 1$ mm, (b) $d = 1.2$ mm, (c) $d = 1.4$ mm.

With the increase in coating thickness, the wave absorption performance of the $\text{Al}_2\text{O}_3\text{-MoSi}_2/\text{Cu}$ coating gradually increased. The coating's thickness was 1.0 mm, reflection loss

was -3.99 dB, absorbing performance was weak at room temperature (25 °C), absorption frequency was at 11 GHz, the coating's reflection loss was -11.69 dB, and the temperature was 700 °C. When the thickness of the $\text{Al}_2\text{O}_3\text{-MoSi}_2/\text{Cu}$ coating was 1.4 mm, the coating's minimum reflection loss was -6.66 dB at 25 °C, and the reflection loss of the coating was -19.09 dB at 700 °C. As can be seen from Figure 8c, the coating thickness is 1.4 mm, the reflection absorption frequency gradually moved to the left as the coating temperature increased, which can be explained by Equation (7) [41]. When the coating thickness was the same, the value of ϵ' increased with the increase in temperature, which moved the frequency band of the interference from high frequency to low frequency so that the coating reached the role of broadband absorption. Parts of the wave-absorbing performance of the coatings are shown in Table 3.

$$f_m = \frac{c}{4d\sqrt{\epsilon_r}} \quad (7)$$

where f_m is the matching frequency, c is the speed of light in vacuum, and d is the thickness of the coating.

Table 3. Different coatings thickness at different temperatures, RL values, and bandwidth.

Thickness (mm)	Temperature (°C)	Minimum RL Values (dB)	Effective Bandwidth (GHz) (RL < -10 dB)
1.0	25	-3.9	-
	400	-8.4	-
	700	-11.69	1.78
1.2	25	-6.2	-
	400	-12.48	2.19
	700	-14.87	2.42
1.4	25	-6.66	-
	400	-13.89	1.68
	700	-19.09	2.83

Cu is often used in electromagnetic shielding material and has good conductivity. The $\text{Al}_2\text{O}_3\text{-MoSi}_2/\text{Cu}$ composite coating does not have good wave absorption performance at room temperature (25 °C) due to the addition of Cu, the coating thickness is 1 mm with a minimum reflection loss of -3.9 dB, as shown in Table 3. According to the XRD pattern in Figure 5, with the increase in temperature, Cu was gradually transformed into Cu_2O , and in a sufficient O_2 environment, Cu_2O was transformed into CuO in the process of heating up in the 700 °C heat preservation test. It can be seen from report [26] that Cu_2O plays a role in improving the absorbing performance of the coating, which is mainly attributed to the conductive network formed by Cu_2O with the increase in temperature. Cu_2O exists on the inner layer of the coating together with $\text{Al}_2\text{O}_3\text{-MoSi}_2$ to increase the electrical conductivity of the coating, which enhances the wave-absorption performance of the coating. In Figure 8c, the coating thickness is 1.4 mm, the minimum reflection loss at 25 °C is only -6.66 dB, but min RL at 700 °C is 19.09 dB. It can be seen from Figure 8 that with the increase in temperature, the coating gradually has good absorbing performance. Specifically, the Cu is transformed into CuO and Cu_2O improves the electrical conductivity of the coating, and improves the wave-absorbing performance of the coating.

The experimental results show that the $\text{Al}_2\text{O}_3\text{-MoSi}_2/\text{Cu}$ absorbing coating by plasma spraying in this work is a new type of absorbing coating used at high temperature, and copper oxide has an influence on the absorbing performance of the coating. Therefore, compared to other wave absorbing coatings, the $\text{Al}_2\text{O}_3\text{-MoSi}_2/\text{Cu}$ coating's wave absorption performance is not obvious at room temperature of 25 °C, but it has good wave absorption performance at high temperatures of 700 °C. The characteristics of wave-absorbing performance with temperature variation deserve attention in future.

4. Conclusions

The results show that the wave absorption performance of the $\text{Al}_2\text{O}_3\text{-MoSi}_2/\text{Cu}$ composite high temperature-resistant coating is gradually enhanced with the increase in temperature. This study conducted the XRD analysis of mixed powder elements and composite coating compounds, and SEM to observe the structure of the composite coating. The SEM micrograph showed that copper oxide exists on the coating surface. The vector network analyzer measured the dielectric properties and calculated Reflection Loss under different temperatures. It was found that Cu_2O formed by Cu at high temperatures can enhance the coating's absorbing properties. Coating thickness was 1.4 mm with the best reflection loss. The coating's reflection loss was -19.09 dB at a temperature of 700 °C and frequency of 10.5 GHz. The results show that the coating has a good high-temperature microwave absorbing performance in the X-band.

Author Contributions: Conceptualization, C.G. and W.X.; methodology, C.G.; formal analysis, Y.J.; investigation, C.G.; data curation, W.X.; writing—original draft preparation, C.G. and Y.J.; writing—review and editing, D.C.; visualization, Y.J.; supervision, D.C.; project administration, J.X.; funding acquisition, J.X. All authors have read and agreed to the published version of the manuscript.

Funding: Guangxi S & T Program (No. AD18126024).

Institutional Review Board Statement: Not applicable.

Informed Consent Statement: Not applicable.

Data Availability Statement: Data is included in this article.

Conflicts of Interest: The authors declare no conflict of interest.

References

1. Liu, H.; Tian, H.; Cheng, H. Dielectric properties of SiC fiber-reinforced SiC matrix composites in the temperature range from 25 to 700 °C at frequencies between 8.2 and 18 GHz. *J. Nucl. Mater.* **2013**, *432*, 57–60. [\[CrossRef\]](#)
2. Gao, H.; Luo, F.; Wen, Q.; Jia, H.; Zhou, W.; Zhu, D. Enhanced high-temperature dielectric and microwave absorption properties of SiC fiber-reinforced oxide matrix composites. *J. Appl. Polym. Sci.* **2018**, *136*, 47097. [\[CrossRef\]](#)
3. Li, M.; Yin, X.; Zheng, G.; Chen, M.; Tao, M.; Cheng, L.; Zhang, L. High-temperature dielectric and microwave absorption properties of $\text{Si}_3\text{N}_4\text{-SiC/SiO}_2$ composite ceramics. *J. Mater. Sci.* **2014**, *50*, 1478–1487. [\[CrossRef\]](#)
4. Song, W.; Cao, M.-S.; Hou, Z.-L.; Yuan, J.; Fang, X.-Y. High-temperature microwave absorption and evolutionary behavior of multiwalled carbon nanotube nanocomposite. *Scr. Mater.* **2009**, *61*, 201–204. [\[CrossRef\]](#)
5. Wan, F.; Yan, J.; Xu, H. Improved mechanical and high-temperature electromagnetic wave absorption properties of SiCf/BN/AlPO₄ composites with absorber multiwalled carbon nanotubes. *Compos. Interfaces* **2020**, 1–18. [\[CrossRef\]](#)
6. Yuan, J.; Yang, H.-J.; Hou, Z.-L.; Song, W.; Xu, H.; Kang, Y.-Q.; Jin, H.-B.; Fang, X.-Y.; Cao, M.-S. Ni-decorated SiC powders: Enhanced high-temperature dielectric properties and microwave absorption performance. *Powder Technol.* **2013**, *237*, 309–313. [\[CrossRef\]](#)
7. Mu, Y.; Zhou, W.; Hu, Y.; Wang, H.; Luo, F.; Ding, D.; Qing, Y. Temperature-dependent dielectric and microwave absorption properties of SiC /SiC- Al_2O_3 composites modified by thermal cross-linking procedure. *J. Eur. Ceram. Soc.* **2015**, *35*, 2991–3003. [\[CrossRef\]](#)
8. Dou, Y.-K.; Li, J.B.; Fang, X.-Y.; Jin, H.-B.; Cao, M.-S. The enhanced polarization relaxation and excellent high-temperature dielectric properties of N-doped SiC. *Appl. Phys. Lett.* **2014**, *104*, 052102. [\[CrossRef\]](#)
9. Micheli, D.; Marchetti, M.; Pastore, R.; Vricella, A.; Gradoni, G.; Moglie, F.; Primiani, V.M. Shielding effectiveness of carbon nanotube reinforced concrete composites by reverberation chamber measurements. In Proceedings of the International Conference on Electromagnetics in Advanced Applications (ICEAA), Torino, Italy, 7–11 September 2015.
10. Chen, D.; Luo, F.; Zhou, W.; Zhu, D. Effect of Temperature on Microwave-Absorption Property of Plasma-Sprayed $\text{Ti}_3\text{SiC}_2/\text{NASICON}$ Coating. *J. Electron. Mater.* **2019**, *48*, 1506–1510. [\[CrossRef\]](#)
11. Zhou, L.; Chen, M.; Dong, Y.; Yuan, Z.; Johnson, D. Enhanced dielectric and microwave absorption properties of Cr/ Al_2O_3 coatings deposited by low-power plasma spraying. *J. Am. Ceram. Soc.* **2016**, *100*, 620–626. [\[CrossRef\]](#)
12. Jia, H.; Zhou, W.; Nan, H.; Qing, Y.; Luo, F.; Zhu, D. High temperature microwave absorbing properties of plasma sprayed $\text{La}_{0.6}\text{Sr}_{0.4}\text{FeO}_{3-\delta}/\text{MgAl}_2\text{O}_4$ composite ceramic coatings. *Ceram. Int.* **2020**, *46*, 6168–6173. [\[CrossRef\]](#)
13. Su, J.; Zhou, W.; Liu, Y.; Qing, Y.; Luo, F.; Zhu, D. High-temperature dielectric and microwave absorption property of plasma sprayed $\text{Ti}_3\text{SiC}_2/\text{cordierite}$ coatings. *J. Mater. Sci. Mater. Electron.* **2015**, *27*, 2460–2466. [\[CrossRef\]](#)
14. Pastore, R.; Delfini, A.; Santoni, F.; Marchetti, M.; Albano, M.; Piergentili, F.; Matassa, R. Space Environment Exposure Effects on Ceramic Coating for Thermal Protection Systems. *J. Spacecr. Rocket.* **2021**, 1–7. [\[CrossRef\]](#)

15. Delfini, A.; Pastore, R.; Santoni, F.; Piergentili, F.; Albano, M.; Alifanov, O.; Budnik, S.; Morzhukhina, A.; Nenarokomov, A.; Titov, D.; et al. Thermal analysis of advanced plate structures based on ceramic coating on carbon/carbon substrates for aerospace Re-Entry Re-Useable systems. *Acta Astronaut.* **2021**, *183*, 153–161. [[CrossRef](#)]
16. Huang, Z.; Zhou, W.; Tang, X.; Li, P.; Zhu, J. Dielectric and Mechanical Properties of MoSi₂/Al₂O₃ Composites Prepared by Hot Pressing. *J. Am. Ceram. Soc.* **2010**, *93*, 3569–3572. [[CrossRef](#)]
17. Wu, Z.-H.; Zhou, W.-C.; Luo, F.; Zhu, D.-M. Effect of MoSi₂ content on dielectric and mechanical properties of MoSi₂/Al₂O₃ composite coatings. *Trans. Nonferrous Met. Soc. China* **2012**, *22*, 111–116. [[CrossRef](#)]
18. Zhou, Y.-Z.; Liu, M.; Yang, K.; Zeng, W.; Song, J.-B.; Deng, C.-M.; Deng, C.-G. Microstructure and Property of MoSi₂-30Al₂O₃ Electrothermal Coating Prepared by Atmospheric Plasma Spraying. *J. Inorg. Mater.* **2019**, *34*, 646–652. [[CrossRef](#)]
19. Shang, K.; Wu, Z.-H.; Zhang, L.-P.; Wang, Q.; Zheng, H.-K. Absorbing Performance of MoSi₂/BC Composites Using Bamboo Charcoal Template. *J. Mater. Eng.* **2019**, *47*, 122–128. [[CrossRef](#)]
20. Jiao, D.; Zhong, X.; Xu, W.; Qiu, W.; Liu, M.; Liu, Z.; Li, Z.; Zhang, G. High Temperature Oxidation Behavior of MoSi₂-CoNiCrAlY Composite Coating Prepared by Plasma Spraying. *Rare Met. Mater. Eng.* **2019**, *48*, 1135–1141.
21. Wu, Z.; Zhou, W.; Luo, F.; Zhu, D. Structure and Dielectric Properties of Alumina Coats Containing MoSi₂-Particle Prepared by Atmosphere Plasma Spraying. *Mater. Rep.* **2011**, *25*, 63–65.
22. Moustafa, S.; El-Badry, S.; Sanad, A.; Kieback, B. Friction and wear of copper-graphite composites made with Cu-coated and uncoated graphite powders. *Wear* **2002**, *253*, 699–710. [[CrossRef](#)]
23. Sun, Y.; Feng, C.; Liu, X.; Or, S.W.; Jin, C. Synthesis, characterization and microwave absorption of carbon-coated Cu nanocapsules. *Mater. Res.* **2014**, *17*, 477–482. [[CrossRef](#)]
24. Zhao, B.; Shao, G.; Fan, B.; Zhao, W.; Zhang, R. Preparation and electromagnetic wave absorption properties of novel dendrite-like NiCu alloy composite. *RSC Adv.* **2015**, *5*, 42587–42590. [[CrossRef](#)]
25. Gao, S.; Zhou, N.; An, Q.; Xiao, Z.; Zhai, S.; Shi, Z. Facile solvothermal synthesis of novel hetero-structured CoNi-CuO composites with excellent microwave absorption performance. *RSC Adv.* **2017**, *7*, 43689–43699. [[CrossRef](#)]
26. Gao, S.; Xing, H.; Li, Y.; Wang, H. Synthesis of Cu₂O/multi-walled carbon nanotube hybrid material and its microwave absorption performance. *Res. Chem. Intermed.* **2018**, *44*, 3425–3435. [[CrossRef](#)]
27. Micheli, D.; Pastore, R.; Vricella, A.; Delfini, A.; Marchetti, M.; Santoni, F. Electromagnetic Characterization of Materials by Vector Network Analyzer Experimental Setup. In *Spectroscopic Methods for Nanomaterials Characterization*; Elsevier: Amsterdam, The Netherlands, 2017; pp. 195–236.
28. Singh, P.; Babbar, V.; Razdan, A.; Srivastava, S.; Puri, R. Complex permeability and permittivity, and microwave absorption studies of Ca(CoTi)_xFe_{12-2x}O₁₉ hexaferrite composites in X-band microwave frequencies. *Mater. Sci. Eng. B* **1999**, *67*, 132–138. [[CrossRef](#)]
29. Panwar, R.; Agarwala, V.; Singh, D. A cost effective solution for development of broadband radar absorbing material using electronic waste. *Ceram. Int.* **2015**, *41*, 2923–2930. [[CrossRef](#)]
30. Chen, D.; Luo, F.; Zhou, W.; Zhu, D. Effect of Ti₃SiC₂ addition on microwave absorption property of plasma sprayed Ti₃SiC₂/NASICON coatings. *J. Mater. Sci. Mater. Electron.* **2018**, *29*, 13534–13540. [[CrossRef](#)]
31. Ranjan, A.; Islam, A.; Pathak, M.; Khan, M.K.; Keshri, A.K. Plasma sprayed copper coatings for improved surface and mechanical properties. *Vacuum* **2019**, *168*, 108834. [[CrossRef](#)]
32. Jin-Yuan, M.; Min, L.; Jie, M.; Chun-Min, D.; De-Chang, Z.; Lin, X. Oxidation-resistance of ZrB₂-MoS₂ Composite Coatings Prepared by Atmospheric Plasma Spraying. *J. Inorg. Mater.* **2015**, *30*, 282–286. [[CrossRef](#)]
33. Wang, L.; Fu, Q.; Zhao, F. Improving oxidation resistance of MoSi₂ coating by reinforced with Al₂O₃ whiskers. *Intermetallics* **2018**, *94*, 106–113. [[CrossRef](#)]
34. Majumdar, S. Formation of MoSi₂ and Al doped MoSi₂ coatings on molybdenum base TZM (Mo-0.5Ti-0.1Zr-0.02C) alloy. *Surf. Coatings Technol.* **2012**, *206*, 3393–3398. [[CrossRef](#)]
35. Ogbuji, L.U. Oxidation behavior of Cu-Cr environmental barrier coatings on Cu-8Cr-4Nb. *Surf. Coat. Technol.* **2005**, *197*, 327–335. [[CrossRef](#)]
36. Cao, M.-S.; Song, W.; Hou, Z.-L.; Wen, B.; Yuan, J. The effects of temperature and frequency on the dielectric properties, electromagnetic interference shielding and microwave-absorption of short carbon fiber/silica composites. *Carbon* **2010**, *48*, 788–796. [[CrossRef](#)]
37. Correia, N.T.; Ramos, J.J.M. On the cooperativity of the β-relaxation: A discussion based on dielectric relaxation and thermally stimulated depolarisation currents data. *Phys. Chem. Chem. Phys.* **2000**, *2*, 5712–5715. [[CrossRef](#)]
38. Liu, Y.; Luo, F.; Zhou, W.; Zhu, D. Dielectric and microwave absorption properties of Ti₃SiC₂ powders. *J. Alloys Compd.* **2013**, *576*, 43–47. [[CrossRef](#)]
39. Huang, Z.; Zhou, W.; Tang, X.; Zhu, J. Effects of milling methods on the dielectric and the mechanical properties of hot-pressed sintered MoSi₂/Al₂O₃ composites. *J. Alloys Compd.* **2011**, *509*, 1920–1923. [[CrossRef](#)]
40. Atwater, J.E.; Wheeler, R.R., Jr. Complex Permittivities and Dielectric Relaxation of Granular Activated Carbons at Microwave Frequencies between 0.2 and 26 GHz. *Carbon* **2003**, *7*, 1801–1807. [[CrossRef](#)]
41. Shao, T.; Ma, H.; Wang, J.; Feng, M.; Yan, M.; Wang, J.; Yang, Z.; Zhou, Q.; Luo, H.; Qu, S. High temperature absorbing coatings with excellent performance combined Al₂O₃ and TiC material. *J. Eur. Ceram. Soc.* **2020**, *40*, 2013–2019. [[CrossRef](#)]